JOURNAL OF BACTERIOLOGY, May 2011, p. 2312–2321 Vol. 193, No. 9
0021-9193/11/$12.00 doi:10.1128/JB.01355-10

Partial Functional Replacement of CymA by SirCD in *Shewanella oneidensis* MR-1▽§

Carmen D. Cordova,[2] Marcus F. R. Schicklberger,[2]# Yang Yu,[2] and Alfred M. Spormann[1,2]*

Departments of Chemical Engineering[1] and of Civil & Environmental Engineering,[2] Stanford University, Stanford, California

Received 11 November 2010/Accepted 20 February 2011

The gammaproteobacterium *Shewanella oneidensis* MR-1 utilizes a complex electron transfer network composed primarily of *c*-type cytochromes to respire under anoxic conditions a variety of compounds, including fumarate, nitrate, and dimethyl sulfoxide (DMSO), in addition to the minerals Fe(III) and Mn(IV). Central to several respiratory pathways is CymA, a cytoplasmic membrane-bound tetraheme *c*-type cytochrome that functions as the major hydroquinone dehydrogenase. To investigate functional redundancy and plasticity in *S. oneidensis* MR-1 electron transport, we isolated Δ*cymA* suppressor mutants and characterized one biochemically and genetically. Interestingly, in the characterized Δ*cymA* suppressor mutant, respiration of fumarate, ferric citrate, and DMSO was restored but that of nitrate was not. The suppression was found to be due to transcriptional activation of *sirC* and *sirD*, encoding a periplasmic iron sulfur protein and an integral membrane hydroquinone dehydrogenase, respectively. Biochemical *in vitro* reconstitution experiments confirmed electron transport between formate and fumarate via fumarate reductase by suppressor membrane fractions. The suppression was found to be caused by insertion of an ISSod1 element upstream of the *sirCD* transcriptional start site, generating a novel, constitutively active hybrid promoter. This work revealed that adaptation of an alternative electron transfer pathway from quinol to terminal oxidoreductases independent of CymA occurs rapidly in *S. oneidensis* MR-1.

Utilization of a wide range of electron acceptors, including fumarate, dimethyl sulfoxide (DMSO), nitrate, trimethyl-*N*-amine oxide (TMAO), manganese oxides, and ferric oxides, in the dissimilatory metal-reducing bacterium (DMRB) *Shewanella oneidensis* MR-1 is mediated by a complex respiratory network. This network extends electron transfer from the cytoplasmic membrane to the periplasm and outer membrane and includes 42 putative *c*-type cytochromes (9, 16, 33, 34). Such *c*-type cytochrome-based electron transport is characteristic of many DMRBs, including *Geobacter*, *Anaeromxyobacter*, and *Shewanella* spp., and reflected in their genome composition (19, 27, 46). The core of an anaerobic electron transport chain in *S. oneidensis* MR-1 involves reduction of quinone by a membrane-associated NADH dehydrogenase and oxidation of quinol by the quinol dehydrogenase CymA, a cytoplasmic membrane-bound tetraheme *c*-type cytochrome. Reduced CymA transfers electrons either to periplasmic terminal reductases, such as fumarate reductase (FccA) or nitrate reductase (NapAB), or to periplasmic *c*-type cytochrome proteins DmsE or MtrA, which extend electron transport to an outer membrane-localized DMSO reductase or OmcA/OmcB (MtrC) Fe(III) reductase, respectively (11, 12, 31).

Despite the abundance of electron transfer components encoded in the *S. oneidensis* MR-1 genome, FccA, NapB, DmsE, and MtrA are believed to directly interact with CymA as the sole quinol dehydrogenase (12, 15, 16, 32, 41, 42). This is in contrast to findings with other *c*-type cytochrome quinol dehydrogenases, such as NapC of *Escherichia coli* and NrfH of *Wolinella succinogenes*, that exhibit a more commonly found high specificity to cognate terminal oxidoreductases, while CymA apparently couples to multiple terminal reductases and periplasmic electron transfer proteins (3, 38). The molecular basis of how CymA functions in transferring to several different oxidoreductases is unknown. Here, we report that the SO0484 gene product (previously annotated as SirD), via a SO0483/0484-encoded quinol dehydrogenase complex (SirCD), can functionally replace the *c*-type cytochrome CymA in several but not all of these respiratory pathways. The SO0484 gene encodes an NrfD/PsrC-like protein, and SO0484 is predicted to encode an integral membrane protein with no associated prosthetic group, while the SO0483 gene encodes a putative periplasmic CooF family iron sulfur protein (8, 45).

Recently, Shirodkar et al. identified SO0479 as encoding the octaheme *c*-type cytochrome SirA, the terminal reductase for sulfite reduction in *S. oneidensis* MR-1, and also showed that deletion of the downstream genes SO0482 to SO0484 contained within a putative 10-gene operon (SO0479 to SO0488) from *S. oneidensis* MR-1 resulted in the inability to reduce sulfite (43). In accordance with the nomenclature in this study, SO0483 and SO0484 are referred to here as *sirC* and *sirD*, respectively. Similar organization of genes encoding SirA homologs in other bacteria has been documented (i.e., *mccA* in *W. succinogenes*), and it has been suggested that the corresponding quinol dehydrogenase encoded by downstream genes (i.e., SO0483 and SO0484 in *S. oneidensis* MR-1) may directly couple to SirA and MccA, respectively (17, 18, 43, 45). SirD and other members of the NrfD/PsrC family, in association

* Corresponding author. Mailing address: Depts. of Chemical Engineering and of Civil and Environmental Engineering, Clark Center E250, 318 Campus Drive, Stanford University, Stanford, CA 94305. Phone: (650) 723-3668. Fax: (650) 724-4927. E-mail: spormann@stanford.edu.

Present address: Institut für Mikrobiologie Universität Freiburg, Schaenzlestr. 1, 79104 Freiburg, Germany.

§ Supplemental material for this article may be found at http://jb.asm.org/.

▽ Published ahead of print on 4 March 2011.

TABLE 1. Strains used in this study

Strain mutation and/or designation	Strain	Relevant genotype	Relevant phenotype[a]			Reference or source
			Fumarate	Nitrate	DMSO	
WT (AS84)	*Shewanella oneidensis* MR-1	*thrB1004 pro thi rpsL hsdS lacZ*DM15	+	+	+	49a
Δ*cymA* (AS435)	*Shewanella oneidensis* MR-1	Δ*cymA*	−	−	−	15
Δ*cymA*^{s} (AS747)	*Shewanella oneidensis* MR-1S$^{\Delta cymA}$	Δ*cymA* 504749::*ISSod1*	+	−	+	This study
AS753	*Escherichia coli* WM3064 pDS3.0-*sirCD*	*thrB1004 pro thi rpsL hsdS lacZ*DM15 RP4–1360 (*araBAD*)*567 dapA1341*::[*erm pir*(wt)]	ND	ND	ND	This study, 49b
Δ*sirCD* (AS754)	*Shewanella oneidensis* MR-1$^{\Delta sirCD}$	Δ*sirCD*	+	+	+	This study
Δ*cymA*^{s} Δ*sirCD* (AS755)	*Shewanella oneidensis* MR-1S$^{\Delta cymA \Delta sirCD}$	Δ*cymA* Δ*sirCD* 504749::*ISSod1*	−	−	−	This study
Δ*cymA*^{s*} (AS756)	*Shewanella oneidensis* MR-1S(II)$^{\Delta cymA}$	Δ*cymA* 504748::*ISSod1*	+	−	+	This study
Δ*cymA*^{s*} Δ*sirCD* (AS758)	*Shewanella oneidensis* MR-1S(II)$^{\Delta cymA \Delta sirCD}$	Δ*cymA* Δ*sirCD* 504748::*ISSod1*	−	−	−	This study
WT pJD (AS763)	*Shewanella oneidensis* MR-1	pJD	ND	ND	ND	This study, 18a
WT pJD*IS* (AS765)	*Shewanella oneidensis* MR-1	pJD*IS*	ND	ND	ND	This study
WT pJD*IS*^{t} (AS766)	*Shewanella oneidensis* MR-1	pJD*IS*^{t}	ND	ND	ND	This study
Δ*cymA*$^{s+}$ (AS767)	*Shewanella oneidensis* MR-1S	AS755 with chromosomal insertion of *sirCD*	+	−	+	This study
WT pJD*IS*^{RE} (AS768)	*Shewanella oneidensis* MR-1	pJD*IS*^{RE}	ND	ND	ND	This study
WT pJD*IS*^{RE*} (AS769)	*Shewanella oneidensis* MR-1	pJD*IS*^{RE*}	ND	ND	ND	This study
AS772	*Escherichia coli* WM3064 pGP704_*sirC*	Noted above	ND	ND	ND	This study
AS773	*Escherichia coli* WM3064 pGP704_*sirD*	Noted above	ND	ND	ND	This study
AS774	*Escherichia coli* WM3064 pGP704_*sirC*$_{his}$	Noted above	ND	ND	ND	This study
AS781	*Escherichia coli* WM3064 pGP704_*sirC*$_{his}$ Δ*sirD*	Noted above	ND	ND	ND	This study
AS789	*Escherichia coli* WM3064 pDS3.0_*sirC*^{wt}/*sirD*^{wt}	Noted above	ND	ND	ND	This study
Δ*cymA*^{s} Δ*sirC* (AS811)	*Shewanella oneidensis* MR-1	Δ*cymA* Δ*sirC* 504749::*ISSod1*	−	−	−	This study
Δ*cymA*^{s} Δ*sirD* (AS812)	*Shewanella oneidensis* MR-1	Δ*cymA* Δ*sirD* 504749::*ISSod1*	−	−	−	This study
Δ*cymA*^{s} *sirC*(His) (AS813)	*Shewanella oneidensis* MR-1	Δ*cymA* 504749::*ISSod1 sirC*(His)	+	ND	ND	This study
Δ*cymA*^{s} Δ*sirD sirC*(His) (AS815)	*Shewanella oneidensis* MR-1	Δ*cymA* Δ*sirD* 504749::*ISSod1 sirC*(His)	−	ND	ND	This study

[a] +, positive; −, negative; ND, not determined.

with a iron-sulfur redox partner, have been hypothesized or shown to couple to a terminal reductase, including the structurally characterized polysulfide reductase complex PsrCBA from *Thermus thermophilus* (22). However, to our knowledge, the substitution of CymA by SirC and SirD is the first time that a member of the NrfD/PsrC family of quinol dehydrogenases can function as an electron relay in an extended electron transport network (44).

In addition to the large number of *c*-type cytochromes and other electron transfer enzymes in the extensive respiratory network of *S. oneidensis* MR-1, its genome also contains an unusually high number (>200) of insertion sequences (IS) (2, 10, 39). Several IS subgroup types present in *S. oneidensis* MR-1, including ISSod1, are associated with IS families that have been shown to contain a −35 hexamer and a −10 hexamer nucleotide sequence in their conserved right and left ends, respectively (4). For integrated IS elements, transcriptional activation of adjacent, non-IS genes can arise due to the outward-directed −35 hexameric nucleotide sequence in conjunction with a local −10 hexameric nucleotide sequence (24, 25). Here we show that IS-mediated expression of the *sirCD* genes resulted in partial functional substitution of CymA by SirCD.

MATERIALS AND METHODS

Growth conditions and media. *E. coli* strains were grown in Luria broth (LB) medium at 37°C. *S. oneidensis* MR-1 strains are described in Table 1 and were grown at 30°C in LB medium or minimal medium (4M) supplemented with 50 mM sodium lactate. When required for growth under anoxic conditions, minimal medium was supplemented with 50 mM sodium fumarate, 50 mM DMSO, 5 mM sodium nitrate, or 25 mM ferric citrate. Anaerobic cultures were prepared in 125-ml serum bottles and treated as previously described (15). Cells for fractionation were grown first in LB medium overnight (~12 h) and then resuspended in anoxic minimal medium containing lactate as an electron donor and carbon source and fumarate as an electron acceptor and were incubated for 4 h before harvesting. If necessary, 2,6-diaminopimelic acid (100 μg ml^{-1}), kanamycin (50 μg ml^{-1}), tetracycline (10 μg ml^{-1}), and gentamicin (10 μg ml^{-1}) were added to the medium. Growth was determined by optical density measurements (A_{600}). Growth experiment data and subsequent analysis are presented using Prism version 4 (Graphpad Software, La Jolla, CA). For ferric iron assays and CFU measurements, a linear scale is shown to indicate correlation between reduced iron levels and CFU counts.

Determination of CFU and iron reduction measurements. From *S. oneidensis* MR-1 cultures grown in 4M minimal medium with 50 mM lactate and 25 mM ferric citrate, two parallel 1-milliliter samples were taken at the corresponding time points. CFU were counted as described by Gescher et al. (15), and ferrous iron was determined using the ferrozine assay described by Ruebush et al. (40).

Mutant construction: *sirC*, *sirD*, and *sirCD* deletions and affinity tag insertions into the genome of *S. oneidensis* MR-1. Strains containing a Δ*sirC*, Δ*sirD*, *or* Δ*sirCD* mutation or affinity tag insertion were constructed according to the protocol of Thormann et al. with minor modifications (48). All primers used in this research are described in Table SA1 in the supplemental material. Primers 1, 2, 3, and 4 were used to amplify 500-bp regions upstream of *sirC* and downstream of *sirD*. These fragments were then ligated after digestion of an introduced EcoRI site and cloned into the SmaI site of pDS3.0 (13), resulting in pDS3.0_*sirCD*. Primers 1, 5, 6, and 7 were used to construct pGP704_*sirC*, and primers 4, 8, 9, and 10 were used for the construction of pGP704_*sirD*. For construction of the knock-in construct pDS3.0_*sirC*(Wt)/*sirD*(Wt), primers 1 and 4 were used to amplify the entire region. The vector pGP704_*sirC*(His) was made using primers 7, 8, 11, and 12. A C-terminal histidine tag was introduced via overlapping PCR extension between an ~500-bp upper fragment and an

~500-bp lower fragment. The same cloning procedure was used for construction of pGP704_*sirC*(His)_Δ*sirD* (with primers 4, 8, 12, and 13). WM3064 was used as the conjugal donor strain for the mating with *S. oneidensis* MR-1 strains as described previously (50).

Cell fractionation. Membrane fractions were prepared as previously reported (15) with minor modifications. Fresh cell pellets were suspended in an equal volume of 100 mM HEPES, pH 7.5, containing 0.1 mg ml^{-1} DNase I and 0.4 mg ml^{-1} lysozyme. Membrane fractions were resuspended in 100 mM HEPES, pH 7.5. For isolation of the *S. oneidensis* MR-1 periplasmic fraction, the following procedure based on a previous study (36) was used. Whole cells were resuspended in 20 mM HEPES, pH 7.5 (0.4 g ml^{-1}). Polymyxin B (Sigma-Aldrich, St. Louis, MO) was added (1 mg ml^{-1}) to the wet cell suspension, and the sample was incubated at 30°C for 1 h. The sample was then centrifuged at 15,000 × *g* for 45 min, and the resulting soluble fraction was defined as the periplasmic fraction. Liquid chromatography-tandem mass spectroscopy (LC-MS/MS) analysis, including identification of protein hits, was conducted by the Stanford University Mass Spectrometry (SUMS) core research facility.

Purification of FccA. The following simplified purification procedure was developed based on a previous study (28). Enriched periplasmic fraction in 10 mM Tris buffer, pH 8.4, was loaded onto a DEAE HiTrap FF column (GE Healthcare, Piscataway, NJ). The column was washed with 8 column volumes of 10 mM Tris buffer, pH 8.4. The column was washed subsequently with 10 column volumes with the same buffer containing 50 mM NaCl. FccA was eluted with buffer containing 125 mM NaCl. Several fractions were collected, and pure fractions were pooled upon analysis via SDS-PAGE.

UV/visible spectroscopy of FccA. Absorption spectra of purified FccA (7 μM) were recorded in anoxic, rubber stopper-sealed quartz cuvettes using a Cary 50 Bio UV-Vis spectrophotometer. FccA as isolated from ion-exchange chromatography was considered to be in the oxidized state. Preparation of all sealed vials containing reagents/buffers and anoxic cuvettes with protein samples were carried out in an anoxic glove box (N_2:H_2, 90%:10%). Reactions were initiated by addition of 10 mM formate where indicated using Hamilton syringes. One milligram of membrane fraction from the wild-type (WT) strain or the Δ*cymA*^{s} mutant suspended in anoxic 100 mM HEPES, pH 7.5, was added. Heme content of ~4 μmol per μmol protein was calculated for FccA using an extinction coefficient of 15.9 mM^{-1} cm^{-1} (523 nm) as reported by Morris et al.

Immunodetection of SirC(His) content in membrane fractions. For detection of SirC(His) through immunoblotting, fractions were run on 15% SDS polyacrylamide gels and blotted onto a nitrocellulose membrane (Bio-Rad Laboratories, Hercules, CA) using a TE 70 semidry transfer blot (GE Healthcare, Piscataway, NJ) according to the manufacturer's instructions. Blots were visualized using the AP detection kit (IBA Bio, Goettingen, Germany) after treatment with mouse monoclonal tetra-His antibody (Qiagen) and goat anti-mouse IgG AP conjugate secondary (Fisher Scientific, Pittsburgh, PA) according to the manufacturer's instructions.

Reverse transcription (RT)-PCR for detection of *sirC*(His) expression. Primers 38 and 52 were used to amplify the entire DNA fragment from the end of *nrfG* to the end of the 3′ extension (His tag) of *sirC*(His) in the Δ*cymA*^{s} *sirC*(His) and Δ*cymA*^{s} Δ*sirD sirC*(His) mutant strains. cDNA (50 ng) was used for amplification.

RNA extraction and cDNA synthesis. Total RNA was isolated from triplicate samples using the enzymatic lysis and mechanical shearing protocol with RNAprotect Bacteria (Qiagen, Valencia, CA), lysozyme (Sigma-Aldrich, St. Louis, MO), acid-washed glass beads (Sigma-Aldrich, St. Louis, MO), and an RNeasy minikit (Qiagen, Valencia, CA) according to the manufacturer's instructions. RNA samples were treated with DNase I amplification grade (Invitrogen, Carlsbad, CA) according to the manufacturer's instructions to remove genomic DNA, with subsequent purification performed with an RNeasy minikit (Qiagen, Valencia, CA). Electrophoretic analysis was performed with an Agilent 2100 bioanalyzer (Agilent Technologies Inc., Palo Alto, CA), and A_{260}/A_{280} ratios were used to assess RNA integrity. Absence of PCR amplification of a genomic region of 100 bp using primers and Phire polymerase (NEB, Ipswich, MA) according to the manufacturer's instructions was determined for verification of the lack of genomic contamination. Using SuperScript III reverse transcriptase (Invitrogen, Carlsbad, CA), cDNA synthesis from total RNA was carried out according to the manufacturer's instructions. Reverse transcription control reactions were performed on triplicate samples with and without reverse transcriptase enzyme.

Quantitative PCR (qPCR) was performed with the following primer pairs (see Table SA1 in the supplemental material): 14/15, 16/17, 18/19, 20/21, 22/23, and 24/25 for SO3186, *sirC*, *sirD*, *sirJ*, *recA*, and *gyrB*, respectively, using equal amounts of cDNA (added in 1 μl volume to a 25-μl reaction) for amplification of each gene region (100 bp). Triplicate reactions were run on a single qPCR experiment using iQ Sybr green super mix (Bio-Rad Laboratories, Hercules, CA). All reactions were performed with the following program: 95.0°C for 3 min, 50 cycles of 95.0°C for 30 s, 55.0°C for 30 s, and 72.0°C, and a melt curve to determine primer specificity: 95.0 for 1 min, 55.0 C for 1 min, and 80 cycles of a stepwise increase by 0.5°C starting at 55.0°C for 10 s. PCR amplification and detection were conducted in an iCycler (Bio-Rad Laboratories, Hercules, CA). Each real-time PCR was performed in triplicate based on three independent RNA extractions. An 100-bp fragment from the *dnaK* gene (amplified from genomic DNA using primers 26 and 27) was amplified using primers 28 and 29 and used for derivation of the standard curve. Expression ratios are given as the $\log_2$ fold difference in quantity of product from the experimental samples (the Δ*cymA*^{s} strain) versus that from the control samples (WT). Normalization of all expression ratios was conducted using normalization factors generated through amplification of three internal control genes (*gyrB*, *dnaK*, and *recA*) analyzed with geNORM (49).

Amplification of insertion site. Primers 30 and 35 were used to amplify the region flanking the insertion site in the WT strain and in the Δ*cymA* mutant, the Δ*cymA* mutant carrying a suppressor (the Δ*cymA*^{s} strain), and the Δ*cymA* mutant carrying the same suppressor and an additional suppressor (the Δ*cymA*^{s*} strain).

mRNA transcript length analysis via PCR. PCR was performed using 60 ng of cDNA from the Δ*cymA*^{s} mutant prepared as stated above. The primer pairs 31/32, 32/33, 34/35, 36/37, 38/39, and 40/41 were used to amplify overlapping regions spanning the region from the 3′ end of ISSod1 to SO0485 in the Δ*cymA*^{s} mutant. Genomic DNA from the Δ*cymA*^{s} mutant was used as a control for all PCRs.

Promoter prediction. Virtual Footprint version 3.0 was used to identify putative −10 regions recognized by sigma 70 using a specific weight position matrix (*E. coli* based) (http://www.prodoric.de/vfp/) (29). The BPROM bacterial promoter predictor was used to identify entire (−35/−10) putative promoter regions (SoftBerry, Mt. Kisco, NY). *E. coli*-based predictions were deemed suitable due to the recent study of single-molecule characterization of the sigma 70 transcription factor of *S. oneidensis* MR-1 indicating that it recognizes −35/−10 regions with a motif similar to that of *E. coli* (14).

Putative ISSod1 promoter fusions to *lacZ* and promoter activity assay. The *lacZ* gene was amplified from *E. coli* genomic DNA using primers 42 and 43. The resulting fragment and pME6041 were then digested using PstI and SphI (NEB, Ipswich, MA) and ligated. Primers 44 and 45 were used to introduce an XbaI site between the SphI and the start codon of the *lacZ* gene. The pME6041 vector containing the *lacZ* gene, renamed pJD, was further modified as follows. A 500-bp region spanning the 3′ end of ISSod1 and the upstream region before the start codon of SO0480 was amplified using primers 46 and 47 to create pJD*IS*. Primer 47 included a ribosome binding site (RBS) upstream of *mxdA* (47). The ISSod1 region was excluded via amplification of the region using primers 47 and 48 to generate pJD*IS*^{t}. The ISSod1 region was truncated to a 50-bp region using primers 47 and 49 to create pJD*IS*^{RE}. The pJD vector and the resulting fragments were digested using SphI and XbaI (NEB) and ligated. A site-directed mutagenesis of a putative −35 hexamer in the 50-bp region construct was made via amplification of the entire vector using primers 50 and 51 followed by ligation and transformation to generate pJD*IS*^{RE*}. A beta-galactosidase assay was performed as described in a previous study with minor modifications (51). Wild-type cells containing each construct were harvested at an optical density at 600 nm (OD_{600}) of ~0.7, and a 20-μl aliquot from each culture was added to 80 μl of permeabilization solution (80 mM dibasic sodium phosphate [Na_2HPO_4], 20 mM KCl, 2 mM $MgSO_4$, 0.8 mg/ml hexadecyltrimethylammonium bromide, 0.4 mg/ml sodium deoxycholate, 5.4 μl/ml beta-mercaptoethanol). Samples were prewarmed to 30°C, and then 600 μl substrate solution (60 mM Na_2HPO_4, 40 mM NaH_2PO_4, 1 mg/ml ONPG, 2.7 μl/ml beta-mercaptoethanol) was added. After samples were incubated for 45 min, the reaction was stopped with 700 μl 1 M sodium carbonate. Calculations were made using the previously described formula.

Images. Images were created using Geneious (version 4.8; A. J. Drummond et al.; Biomatters, Auckland, New Zealand) and Inkscape (version 0.47; http://www.inkscape.org).

RESULTS

Identification of extragenic suppressors of a Δ*cymA* mutation. The goal of this study was to probe for plasticity of *S. oneidensis* MR-1 electron transfer components to substitute for the quinol dehydrogenase CymA in mediating electron transport from the single quinol pool to several different respiratory

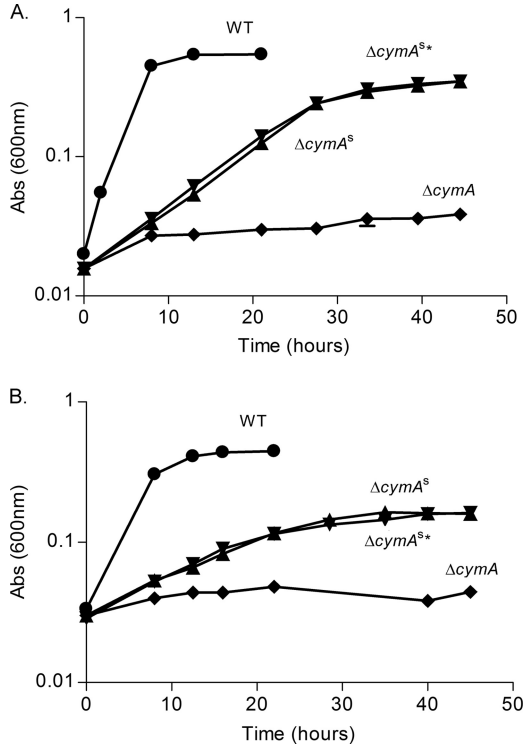

FIG. 1. Anaerobic growth of Δ*cymA* suppressor strains (Δ*cymA*^{s} and Δ*cymA*^{s*}) in 4M minimal medium supplemented with 50 mM lactate and 50 mM DMSO (A) or 50 mM fumarate (B). Symbols: ●, WT strain; ▲, Δ*cymA*^{s} strain; ▼, Δ*cymA*^{s*} strain; ◆, Δ*cymA* strain. Growth is indicated by optical density at 600 nm [Abs (600nm)].

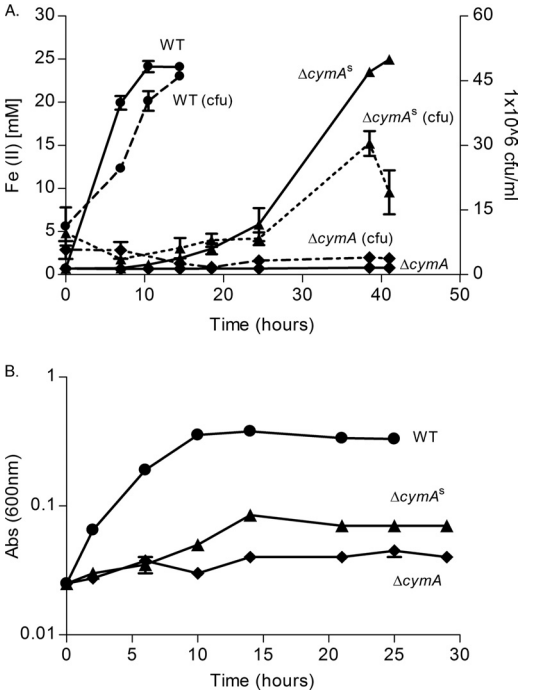

FIG. 2. Anaerobic growth of strain Δ*cymA*^{s} in 4M minimal medium supplemented with 50 mM lactate and 25 mM ferric citrate (A) and 5 mM nitrate (B). Symbols: ●, WT strain; ▲, Δ*cymA*^{s} strain; ◆, Δ*cymA* strain. Dashed lines in panel A represent CFU/ml counts, while solid lines represent reduced Fe(II). Optical density at 600 nm [Abs (600nm)] was measured to determine growth in panel B.

pathways. Serum vials containing anoxic 4 M minimal medium supplemented with 50 mM lactate as the electron donor and 50 mM fumarate as the electron acceptor were inoculated in triplicate with the Δ*cymA* strain. After an incubation of 13 days, turbidity appeared in one of the serum vials, and aliquots were plated on LB plates for isolation of apparent suppressor mutants. After microbiological purification, one suppressor strain, referred to as the Δ*cymA*^{s*} mutant, was retained and characterized for growth. The Δ*cymA*^{s} mutant grew anaerobically using fumarate, DMSO, and ferric citrate as the electron acceptor; however, growth with nitrate as the electron acceptor was significantly attenuated (Fig. 1, data not shown). These growth phenotypes were indistinguishable from those of another suppressor mutant, the Δ*cymA*^{s*} mutant, that we had isolated earlier during this study under the same conditions (Fig. 2). The Δ*cymA*^{s} and Δ*cymA*^{s*} strains both had growth rates of ~0.08 h^{-1} compared to ~0.24 h^{-1} for the WT strain with fumarate or DMSO as the electron acceptor, indicating ~3-fold faster growth by the WT. The parental strain of the Δ*cymA*^{s} mutant, obtained from earlier experiments, carried a Δ*cymA* mutation and a truncated, nonfunctional *cymA* allele with the insertion sequence ISSod9 integrated after nucleotide 57 (relative to the translational start site of *cymA*) in pBAD*cymAH1* (data not shown). Loss of the plasmid after 10 serial transfers and microbiological purification was confirmed by antibiotic sensitivity and PCR analysis and did not affect the suppressor phenotype (data not shown). These findings showed that extragenic suppressors of a Δ*cymA* mutation can be obtained in *S. oneidensis* MR-1.

Identification of enhanced expression of *sirCD* in the Δ*cymA*^{s} strain. To identify genes involved in the suppression of the Δ*cymA* mutation, protein composition in the membranes and periplasm was determined in the Δ*cymA*^{s} strain as this suppressor was isolated and pursued prior to isolation of the Δ*cymA*^{s*} strain. Both the Δ*cymA*^{s} mutant and the WT strain were cultured under fumarate-respiring conditions, harvested at mid-log phase, and fractionated to isolate the periplasmic and membrane fractions. Figure 3 shows the Coomassie-stained protein profiles of the membrane and periplasmic fractions, revealing different band patterns in both fractions in the WT and Δ*cymA*^{s} strains. We focused on one prominent protein band (~17 kDa) in the periplasmic fraction of the Δ*cymA*^{s} strain which was absent in the wild type. In order to identify the protein(s) contained in the band, the gel section was excised, in-gel trypsin digested, and subjected to LC-MS/MS analysis. The resulting MS/MS data were searched against all proteins encoded by the *S. oneidensis* MR-1 genome. The most abundant protein in the 17-kDa protein band, according to total peptides identified (43), was SirJ (previously annotated as NosL) (see Table SA2 in the supplemental material). *sirJ* (SO0485) is a gene in a cluster including *sirK*, *sirL*, and *sirM*, previously annotated as *nosDFY*, which are required for the assembly of the copper-containing active site in nitrous oxide reductase in *E. coli* (26, 52). Sequence analysis of *S. oneidensis* MR-1 has not revealed the presence of nitrous oxide reductase (9). We identified, however, upstream of *sirJ*, a SO0483/0484

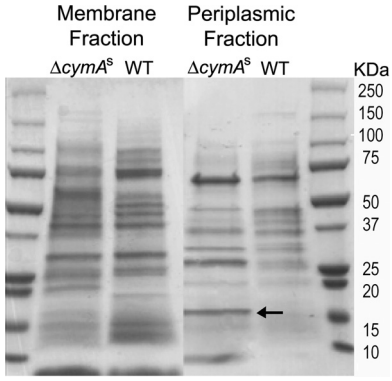

FIG. 3. Coomassie-stained SDS-PAGE gels of the periplasmic and total membrane fractions from WT and Δ*cymA*^{s} strains. Cells were grown anaerobically in 4 M minimal medium with 50 mM lactate (electron donor) and 50 mM fumarate (electron acceptor) and harvested at mid-log phase. The lanes were loaded with 30 μg of protein. Band sizes of the protein ladder are indicated on the left. The gel band selected for LC-MS/MS analysis is indicated with an arrow.

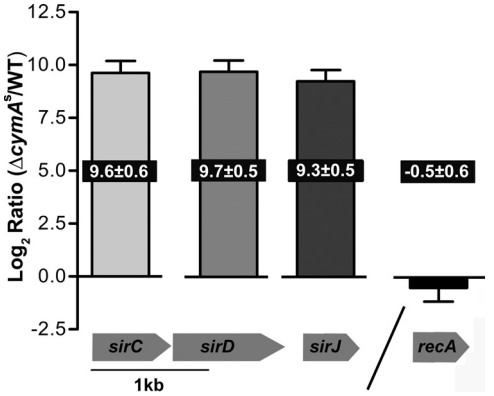

FIG. 4. qRT-PCR-derived expression ratios of *sirC*, *sirD*, *sirJ*, *recA*, and SO3186. Log_2 ratios represent gene expression at mid-logarithmic phase in the Δ*cymA*^{s} strain compared to those in the WT strain. Ratios were normalized as described in Materials and Methods.

(*sirCD*) gene cluster, which was identified previously as a quinol dehydrogenase linked to sulfite reduction. SO0483 (*sirC*) of *S. oneidensis* MR-1, previously annotated as a NrfC-type protein, is a member of the CooF family of iron sulfur proteins, which are involved in anaerobic electron transfer (8). SirC shows sequence similarity to NrfC of *E. coli* K-12 with an expected value of 7×10^{-43} over 226 amino acids. SO0484 (*sirD*) of *S. oneidensis* MR-1 also shows sequence similarity to NrfD from *E. coli* K-12 (expected value, 7×10^{-30} over 307 amino acids). While NrfC and NrfD of *E. coli* are involved in formate-dependent nitrite respiration, past genetic and physiological studies on nitrate and nitrite, as well as the recent study on sulfite reduction in *S. oneidensis* MR-1, have indicated a role for the quinol dehydrogenase encoded by *sirCD* in respiration of sulfur compounds only (12, 43). Nevertheless, we hypothesized that the appearance of SirJ in the periplasmic fraction could have been due to a polar effect resulting from the transcriptional activation of the upstream *sirCD* genes, which may be required for suppression of the Δ*cymA* phenotype. In order to test for such transcriptional activation, WT and Δ*cymA*^{s} strains were grown anaerobically to mid-log phase in 4M medium with fumarate as the electron acceptor, and total RNA was extracted. cDNA was prepared and amplified from the harvested RNA, and mRNA levels of *sirC*, *sirD*, *sirJ* (SO0485), and as controls *dnaK* (SO1126), *gyrB* (SO0011), and *recA* (SO3430) were quantified by qRT-PCR. As shown in Fig. 4, *sirC*, *sirD*, and *sirJ* were significantly upregulated in the suppressor strain (the Δ*cymA*^{s} mutant) and to similar levels (9.6 ± 0.6, 9.7 ± 0.5, and 9.3 ± 0.5, respectively), which suggested that these genes might form a transcriptional unit. In contrast, *recA* expression (-0.5 ± 0.6) shows a minimal difference. Therefore, the level of expression of *sirCD* was elevated in the Δ*cymA*^{s} strain, which suggested a possible role for SirCD in the observed suppression.

Elucidation of *sirCD* genes as essential for the suppressor phenotype. In order to conclusively show that the *sirCD* genes are required for suppression, we constructed in-frame deletions of both genes (Δ*sirCD*) in WT and Δ*cymA*^{s} strains and tested the resulting mutants, the Δ*sirCD* and Δ*cymA*^{s} Δ*sirCD* strains, respectively, for growth. Figure 5a,b shows that deletion of *sirCD* abolished growth on fumarate and DMSO in the Δ*cymA*^{s} Δ*sirCD* strain but not in the Δ*sirCD* strain. Figure 5C and D show that single gene deletion strains, the Δ*cymA*^{s} Δ*sirC* and Δ*cymA*^{s} Δ*sirD* mutants, also showed a loss in growth with either fumarate or DMSO as the electron acceptor, similarly to a Δ*cymA* mutant (AS435). Thus, we concluded that expression of both *sirC* and *sirD* is required for the observed suppression in the Δ*cymA*^{s} strain. Complementation by a knock-in of wild-type *sirCD* into the genome of the Δ*cymA*^{s} Δ*sirCD* strain (resulting in the Δ*cymA*$^{s+}$ strain) restored growth with fumarate and DMSO as an electron acceptor, respectively (see Fig. SA1 in the supplemental material). These data conclusively demonstrated that *sirC* and *sirD* were essential for suppression of the Δ*cymA* mutation.

Immunolocalization of SirC. Since both *sirC* and *sirD* were required for the suppressor phenotype, we hypothesized that *sirCD* encoded a membrane-bound quinol dehydrogenase complex similar to that observed for the polysulfide reductase PsrCBA from *T. thermophilus* and hypothesized for the formate-dependent nitrite quinol dehydrogenase NrfCD from *E. coli* (45). To enable immunodetection of SirC, we introduced a C-terminal His tag as a 3′ extension to *sirC* to form the Δ*cymA*^{s} *sirC*(His) and Δ*cymA*^{s} Δ*sirD* *sirC*(His) mutant strains. Both strains were grown under oxic conditions in 4M medium (with lactate as the electron donor) to the onset of stationary phase; in addition, the Δ*cymA*^{s} *sirC*(His) strain was also grown under fumarate-respiring conditions. All samples were harvested and fractionated to isolate the soluble (cytoplasmic), membrane and periplasmic fractions. Immunodetection of SirC(His) by Western blotting showed that SirC(His) primarily localized to the membrane fraction under fumarate-respiring conditions (Fig. 6A). Under oxic conditions SirC(His) could be detected chromogenically in comparable amounts in the membrane and periplasmic fractions harvested from the Δ*cymA*^{s} *sirC*(His) strain (Fig. 6A). Figure 6B indicates that in the Δ*cymA*^{s} Δ*sirD* *sirC*(His) strain, deletion of *sirD* resulted in a lower level of SirC(His) with only a minimal amount localized to the membrane and not in the periplasmic or soluble (cytoplasmic) fractions. Equal amounts of protein (15 μg) were loaded in all samples. Immunogenic detection of SirC(His) in the Δ*cymA*^{s}

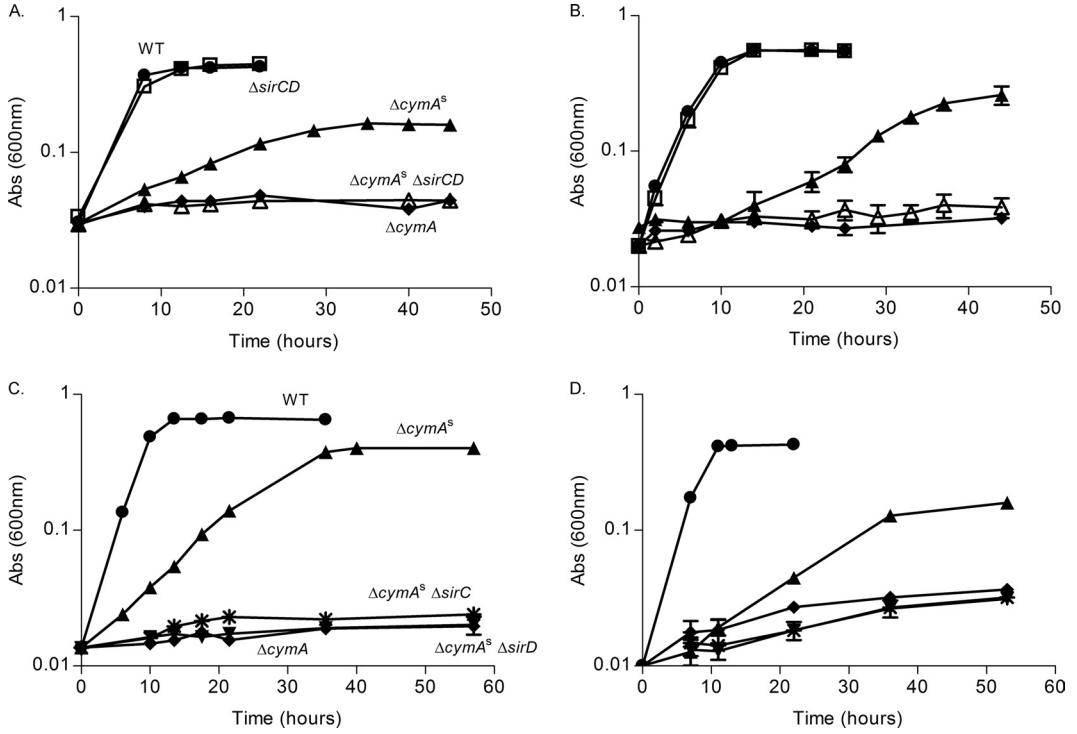

FIG. 5. Effect of Δ*sirC*, Δ*sirD*, *and* Δ*sirCD* deletions on growth with fumarate and DMSO as the electron acceptor in the Δ*cymA*^{s} strain. (A) Growth of WT, Δ*cymA*^{s}, Δ*sirCD*, Δ*cymA*, and Δ*cymA*^{s} Δ*sirCD* strains in 4M minimal medium supplemented with 50 mM lactate (electron donor) and 50 mM fumarate (electron acceptor). (B) DMSO (50 mM) was substituted as the electron acceptor. Growth was measured by optical density at 600 nm [Abs (600nm)]. (C) Growth of WT, Δ*cymA*^{s} Δ*sirC*, Δ*cymA*^{s} Δ*sirD*, Δ*cymA*, and Δ*cymA*^{s} strains with 100 mM lactate and 100 mM fumarate. (D) Growth of WT, Δ*cymA*^{s} Δ*sirC*, Δ*cymA*^{s} Δ*sirD*, Δ*cymA*, and Δ*cymA*^{s} strains with 50 mM lactate and 50 mM DMSO. Symbols: ●, WT strain; □, Δ*sirCD* strain; ▲, Δ*cymA*^{s} strain; Δ, Δ*cymA*^{s} Δ*sirCD* strain; ◆, Δ*cymA* strain; *, Δ*cymA* Δ*sirC* strain; ▼, Δ*cymA* Δ*sirD* strain.

strain (untagged negative control) and RT-PCR of *sirC*(His) in the Δ*cymA*^{s} *sirC*(His) and Δ*cymA*^{s} Δ*sirD sirC*(His) strains indicated that a lower level of SirC(His) was not an artifact of immunodetection or due to lower expression of *sirC*(His) in the Δ*cymA*^{s} Δ*sirD sirC*(His) strain (Fig. 6C). Therefore, these results suggest that expression of *sirD* is required for protein stability of SirC(His), as the level of SirC(His) produced in the Δ*cymA*^{s} *sirC*(His) strain in all fractions under fumarate-respiring conditions or oxic conditions is greater than that observed in the Δ*cymA*^{s} Δ*sirD sirC*(His) strain. However, expression of *sirD* was not an absolute requirement for *sirC* expression.

***In vitro* electron transfer between membranes from Δ*cymA*^{s} and FccA, the fumarate terminal reductase.** In order to directly test for the proposed new electron transfer pathway from the putative quinol dehydrogenase complex encoded by *sirCD* to FccA *in vitro*, we examined whether membrane fractions from the Δ*cymA*^{s} strain could transfer electrons directly to FccA in the absence of other periplasmic oxidoreductase components. Assays were performed using membrane fractions from WT and Δ*cymA*^{s} strains that were prepared under anoxic conditions from fumarate-grown cells. For purification of FccA, WT cells were harvested and treated with the antibiotic polymyxin B in order to permeabilize the outer membrane, thus releasing and enriching for the periplasmic fraction. The resulting protein fraction was then passed over a weak anion-exchange column, and FccA was eluted using a NaCl gradient in 10 mM Tris buffer, pH 8.4. Elution of the protein occurred with 125 mM NaCl (see Fig. SA2 in the supplemental material). We used formate as an *in vitro* electron donor for our electron transfer activity assays similarly to experiments that previously characterized electron transfer to FccA with *S. oneidensis* MR-1 wild-type (CymA) membrane fractions (28). By monitoring the redox status of FccA spectrophotometrically, we found that formate (10 mM), membrane fraction (1 mg), and FccA (7 μM) were required for FccA reduction as revealed by the characteristic absorption maxima of a reduced *c*-type cytochrome at 523 and 552 nm (Fig. 7E and F). Omission of the electron donor formate resulted in an oxidized FccA in the presence of either membrane fraction from the Δ*cymA*^{s} or WT strains (Fig. 7A and B). In the absence of FccA, only weak background absorption of one or more *c*-type cytochrome(s) was observed from both formate-reduced membrane fractions (Fig. 7C and D). FccA was not reduced by formate alone (data not shown). The Δ*cymA* and Δ*cymA* Δ*sirCD* mutants cannot grow using fumarate, and an alternative menaquinone-dependent, CymA-independent electron acceptor is unavailable. As a result, these strains were not suitable as a negative control due to the possible absence of components, including formate dehydrogenase and menaquinone, when grown under differing conditions. Ultimately, these biochemical experiments showed that membrane fractions of the Δ*cymA*^{s} strain containing SirCD could functionally substitute for CymA-containing membrane fractions in an *in vitro* electron transfer pathway from formate to FccA.

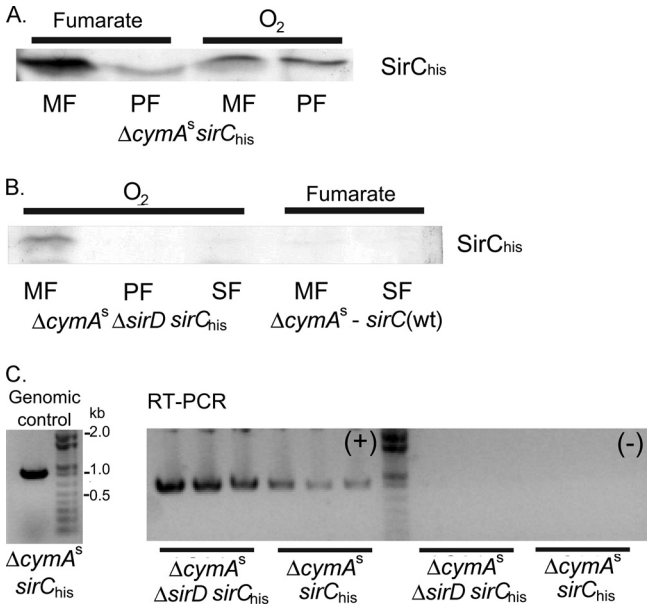

FIG. 6. Immunolocalization of SirC(His) and *sirC*(His) expression in Δ*cymA*^{s} *sirC*(His) and Δ*cymA*^{s} Δ*sirD sirC*(His) strains. The Δ*cymA*^{s} *sirC*(His) and Δ*cymA*^{s} mutant strains were grown with 50 mM lactate in 4M minimal medium with 50 mM fumarate. The Δ*cymA*^{s} *sirC*(His) and Δ*cymA*^{s} Δ*sirD sirC*(His) mutant strains were grown with 50 mM lactate in 4M minimal medium under oxic conditions. Cells were fractionated as described in Materials and Methods for isolation of total membrane (MF), periplasmic (PF), and soluble (cytoplasmic) (SF) fractions. SirC(His) was detected chromogenically using a monoclonal tetra-His antibody. A 15-μg sample of the above fractions was applied to each lane. (A) SirC(His) immunodetection in fumarate and O_2-grown Δ*cymA*^{s} *sirC*(His) strain samples. (B) SirC(His) immunodetection in O_2-grown Δ*cymA*^{s} Δ*sirD sirC*(His) strain samples and fumarate-grown Δ*cymA*^{s} strain samples. (C) RT-PCR of *sirC*(His) in Δ*cymA*^{s} *sirC*(His) and Δ*cymA*^{s} Δ*sirD sirC*(His) strains. Left: PCR amplification from Δ*cymA*^{s} *sirC*(His) genomic DNA (genomic control). Right: RT-PCR amplification of *sirC*(His) is shown using Δ*cymA*^{s} *sirC*(His) and Δ*cymA*^{s} Δ*sirD sirC*(His) RNA samples with (+) and without (−) reverse transcriptase.

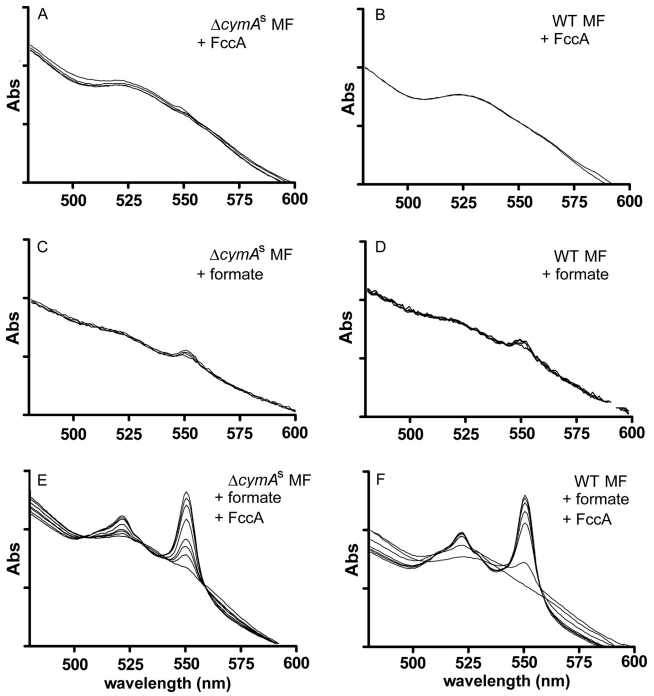

FIG. 7. *In vitro* formate-dependent reduction of terminal fumarate reductase FccA by membrane fractions of Δ*cymA*^{s} and WT strains. UV-visible spectra are shown. (A) FccA (7 μM) and 1 mg membrane fraction (Δ*cymA*^{s} MF). (B) FccA (7 μM) and 1 mg membrane fraction (WT MF). (C) Δ*cymA*^{s} membrane fractions (1 mg) and 10 mM formate (electron donor). (D) WT membrane fractions (1 mg) and 10 mM formate (electron donor). (E) FccA (7 μM), 1 mg membrane fraction (Δ*cymA*^{s} MF), and 10 mM formate. (F) FccA (7 μM), 1 mg membrane fraction (WT MF), and 10 mM formate. Reduction was observed by the presence of specific *c*-type cytochrome peaks for FccA at 523 nm and 552 nm.

Identification of ISSod1-mediated transcriptional activation of *sirCD* as the genetic basis of suppression. Transcriptional activation of *sirCD* has not been observed under CymA dependent-respiring conditions (1). Thus, we reasoned that in the suppressor strains a mutation may have occurred that caused the upregulation of *sirCD*. Sequence analysis of the genomic region spanning genes SO0479 (*sirA*) through *sirD* by PCR analysis revealed that an ISSod1 element had inserted at chromosomal positions 504748 and 504749 within *sirA* in the Δ*cymA*^{s*} and Δ*cymA*^{s} strains, respectively (see Fig. SA3 in the supplemental material). To test whether the IS element was affecting expression of *sirCD*, RT-PCR analysis was used to map the approximate transcriptional start of the operon containing *sirCD* in the Δ*cymA*^{s} strain. Through overlapping PCR amplification of cDNA from the Δ*cymA*^{s} strain, we determined that the mRNA transcript includes the genes SO0480 to *sirJ* (SO0485) and does not include the ISSod1 insertion sequence or the associated terminal reductase gene *sirA* (SO0479) (see Fig. SA4 in the supplemental material).

Based on the observation that ISSod1 was not part of the mRNA transcript yet appeared to be required for suppression, we hypothesized that the insertion sequence contained at least part of a new promoter region required for transcriptional activation of the operon containing *sirCD*. Analysis of the entire region of ISSod1 suggested the presence of a sigma 70-associated promoter element: a putative −35 hexameric nucleotide sequence within the 50-bp conserved right end of IS at an appropriate distance from a genomic region that contains a recognizable −10 hexamer nucleotide sequence. To test whether the region upstream of SO0480, including the ISSod1 right end, had promoter activity, truncations of a 500-bp fragment from the Δ*cymA*^{s} strain (immediately upstream to the translational start site of SO0480 at chromosomal position 504866) were constructed and fused transcriptionally to *lacZ*. Constructs were cloned into pJD and introduced into the WT strain. Promoter activity was detected via beta-galactosidase assays of aerobically grown mid-log-phase cells (OD_{600}, ~0.7). Beta-galactosidase activity of 650 ± 20 Miller units (MU) was measured in cells harboring the entire 500-bp region (pJD*IS*). Deletion of the entire ISSod1 fragment (pJD*IS*^{t}) dramatically reduced beta-galactosidase activity to 24 ± 2 MU, indicating in our assays its requirement for transcription (Fig. 8). Subsequently, we modified the 500-bp promoter region to include only the conserved 50-bp ISSod1 right end region (162 bases total; pJD*IS*^{RE}). We observed a similar degree of activity (610 ± 10 MU) to that of the 500-bp construct containing the

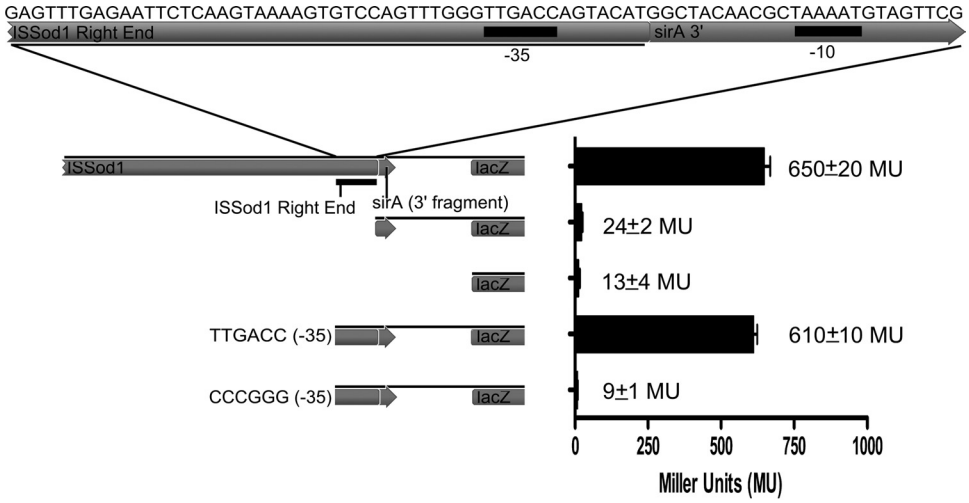

FIG. 8. Insertion of ISSod1 within the 3′ region of *sirA* and identification of a hypothetical hybrid promoter formed at the insertion site. *lacZ* was cloned downstream of several genomic regions containing truncations of ISSod1 and the region upstream of *sirB* (SO0480) in order to test for promoter activities. The constructs are as follows (top to bottom): pJD*IS*, 300-bp right end of ISSod1 and the entire upstream region of SO0480 (*sirB*); pJD*IS*^{t}, upstream region of *sirB* only; pJD, no genomic region (negative control); pJD*IS*^{RE}, 51-bp (conserved) right end of ISSod1 and upstream region of *sirB*; and pJD*IS*^{RE*}, 51-bp ISSod1 right end with a site-directed mutation (TTGACC → CCCGGG) and *sirB* upstream region. WT cells containing each of the constructs on a plasmid were grown to an OD_{600} of ~0.7 and assayed for beta-galactosidase activities. Activity was limited to inclusion of a 50-base region (conserved right end) of ISSod1 and was abolished through a site-directed mutagenesis (TTGACC → CCCGGG). Predicted promoter region is shown.

larger ISSod1 region, and we also observed that the associated activity could be abolished (9 ± 1 MU) through a site-directed mutation of the putative −35 region (TTGACC → CCCGGG; pJD*IS*^{RE*}) (Fig. 8). Taken together, the predicted and observed promoter activity as well as the narrow insertion site confined to a 1-base difference in independently isolated Δ*cymA* suppressor mutants show that insertion of ISSod1 forms a putative hybrid promoter, which leads to transcriptional activation of genes SO0480 to SO0485, including *sirCD.*

DISCUSSION

c-type cytochromes play a critical role in the coupling of the electron transport chain from membrane-bound quinols to terminal oxidoreductases in the outer membrane in *S. oneidensis* MR-1 as well as in other DMRB. Previously, we showed that as members of the same protein family, CymA from *S. oneidensis* MR-1 and NapC from *E. coli* were functionally interchangeable in their activity to transfer electrons to fumarate reductase FccA (15). The results of this work demonstrate that a structurally distinct NrfD/PsrC-type quinol dehydrogenase, SirD, in association with its putative iron sulfur redox partner, SirC, can transfer electrons from quinols to the same respiratory pathways as CymA, except for nitrate (Fig. 9). Our genetic experiments indicate that both *sirC* and *sirD* are required for the growth of the suppressor mutant with the CymA-dependent electron acceptors DMSO and fumarate. Immunodetection localized SirC primarily to the membrane fraction under fumarate-respiring conditions, while under aerobic conditions, SirC is more evenly distributed between the periplasm and membrane fraction. Interestingly, deletion of *sirD* affected the levels of SirC protein but not *sirC* gene expression, suggesting that *sirD* expression is required for SirC stability. Given the evidence of SirC localization to the membrane fraction of Δ*cymA*^{s} cells grown with fumarate, we found that membrane fractions from Δ*cymA*^{s} or wild-type strains could transfer electrons to FccA *in vitro*.

The observed functional complementation of a Δ*cymA* mutation by SirCD, while novel, is not surprising. Common to all members of the NrfD/PsrC family, including PsrC (polysulfide respiration), TtrC (tetrathionate respiration), and NrfD (nitrite respiration) is a predicted or experimentally shown coupling to a CooF family iron sulfur protein (20–22). However, in tetrathionate respiration by *Salmonella enterica* serovar Typhimurium LT2 and polysulfide respiration by *T. thermophilus*, electrons are subsequently transferred to iron sulfur molybdoenzymes. As has also been proposed for the iron sulfur proteins encoded by the *sirC* and *mccC* genes from *S. oneidensis* MR-1 and *W. succinogenes*, respectively, *E. coli* NrfC couples instead to a *c*-type cytochrome protein, NrfB (17, 21, 43). In *E. coli*, NrfD, via the iron sulfur protein NrfC, has been proposed to reduce the pentaheme *c*-type cytochrome NrfB via a putative NrfAB (20-heme) heterotetrameric complex *in vivo* (5, 6). Interestingly, Clarke et al. showed that a truncation of an N-terminal MtrA polypeptide, which shares significant homology and similar heme organization to NrfB from *E. coli*, forms a mature *c*-type cytochrome, supporting the idea that larger cytochromes may be modular extensions of smaller ones (7). Given the documented similarity between heme positioning and possible structural modularity of *c*-type cytochromes, we propose the model shown in Fig. 9, whereby the NrfD/PsrC-type quinol dehydrogenase SirCD transfers electrons either directly or indirectly to the various *c*-type cytochrome containing periplasmic oxidoreductases, including the terminal reductases.

Our results indicate that the transcriptional activation of *sirCD* was the consequence of an insertion sequence-dependent gene activation. Such rare IS element-based transcriptional activation has been documented previously in the up-

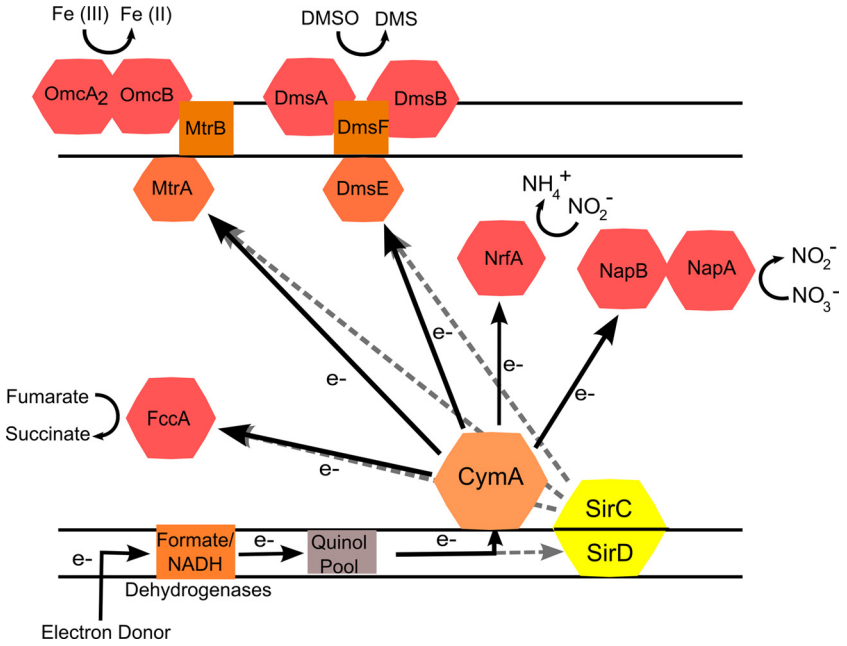

FIG. 9. Model of CymA-dependent (black solid arrows) and the proposed CymA-independent (gray dashed arrows) respiratory pathways in Δ*cymA*^{s} and Δ*cymA*^{s*} strains. See text for details.

regulation of phenol-degrading genes (*pheBA*) in *Pseudomonas* sp. strain EST1001 (23, 35) and in the expression of the silent *bgl* operon in *Escherichia coli* (37). Here, we found that *sirCD* expression was due to the insertion of ISSod1 within the 3′ end of *sirA* and the formation of a putative hybrid promoter. Based on our data, the octaheme terminal reductase SirA as a possible (intermediate) electron acceptor for SirCD is not necessary for the suppression in Δ*cymA*^{s} (Fig. 9). The uncoupling of *sirCD* expression from that of its cognate oxidoreductase and its constitutive expression (observed under oxic and anoxic conditions), closely resembles the unique monocistronic expression of *cymA* and elevated expression under microaerobic conditions, both conditions that have been suggested to allow CymA to transfer electrons to multiple periplasmic oxidoreductases (1, 30). Thus, we propose that the insertion sequence-mediated transcriptional activation led to an alternative route of electron transfer whereby SirCD was accessible to several reductases.

It is important to note that while our experiments showed that expression of *sirCD* is essential for the suppression of a Δ*cymA* mutation, these experiments have not determined the entire set of required genes for the observed suppression or seek to address the overall metabolic efficacy (i.e., difference in growth rates compared to that of the wild type) of suppression in both Δ*cymA* suppressor strains isolated (Fig. 2). Those points we will address in future studies. In addition, the inability of the suppressor strains to grow with nitrate as electron acceptor is an interesting finding and remains unresolved so far.

ACKNOWLEDGMENTS

The research was supported by NSF grant (CHE 0431425) to A.M.S. through the Stanford Environmental Molecular Science Institute.

We thank Sharon R. Long, Gordon E. Brown, Jr., and the Shewanella Federation for insightful discussions.

REFERENCES

1. **Beliaev, A. S., et al.** 2005. Global transcriptome analysis of *Shewanella oneidensis* MR-1 exposed to different terminal electron acceptors. J. Bacteriol. **187:**7138–7145.
2. **Bordi, C., C. Iobbi-Nivol, V. Mejean, and J. C. Patte.** 2003. Effects of ISSo2 insertions in structural and regulatory genes of the trimethylamine oxide reductase of *Shewanella oneidensis*. J. Bacteriol. **185:**2042–2045.
3. **Brondijk, T. H., A. Nilavongse, N. Filenko, D. J. Richardson, and J. A. Cole.** 2004. NapGH components of the periplasmic nitrate reductase of *Escherichia coli* K-12: location, topology and physiological roles in quinol oxidation and redox balancing. Biochem. J. **379:**47–55.
4. **Charlier, D., J. Piette, and N. Glansdorff.** 1982. IS3 can function as a mobile promoter in *E. coli*. Nucleic Acids Res. **10:**5935–5948.
5. **Clarke, T. A., J. A. Cole, D. J. Richardson, and A. M. Hemmings.** 2007. The crystal structure of the pentahaem c-type cytochrome NrfB and characterization of its solution-state interaction with the pentahaem nitrite reductase NrfA. Biochem. J. **406:**19–30.
6. **Clarke, T. A., et al.** 2004. Purification and spectropotentiometric characterization of *Escherichia coli* NrfB, a decaheme homodimer that transfers electrons to the decaheme periplasmic nitrite reductase complex. J. Biol. Chem. **279:**41333–41339.
7. **Clarke, T. A., et al.** 2008. The role of multihaem cytochromes in the respiration of nitrite in *Escherichia coli* and Fe(III) in *Shewanella oneidensis*. Biochem. Soc. Trans. **36:**1005–1010.
8. **Cole, J.** 1996. Nitrate reduction to ammonia by enteric bacteria: redundancy, or a strategy for survival during oxygen starvation? FEMS Microbiol. Lett. **136:**1–11.
9. **Cruz-Garcia, C., A. E. Murray, J. A. Klappenbach, V. Stewart, and J. M. Tiedje.** 2007. Respiratory nitrate ammonification by *Shewanella oneidensis* MR-1. J. Bacteriol. **189:**656–662.
10. **Drouin, F., J. Melancon, and P. H. Roy.** 2002. The IntI-like tyrosine recombinase of *Shewanella oneidensis* is active as an integron integrase. J. Bacteriol. **184:**1811–1815.
11. **Fredrickson, J. K., et al.** 2008. Towards environmental systems biology of *Shewanella*. Nat. Rev. Microbiol. **6:**592–603.
12. **Gao, H., et al.** 2009. Reduction of nitrate in *Shewanella oneidensis* depends on atypical NAP and NRF systems with NapB as a preferred electron transport protein from CymA to NapA. ISME J. **3:**966–976.
13. **Gao, W., et al.** 2006. Knock-out of SO1377 gene, which encodes the member of a conserved hypothetical bacterial protein family COG2268, results in alteration of iron metabolism, increased spontaneous mutation and hydrogen peroxide sensitivity in *Shewanella oneidensis* MR-1. BMC Genomics **7:**76.

14. **Gassman, N. R., et al.** 2009. In vivo assembly and single-molecule characterization of the transcription machinery from *Shewanella oneidensis* MR-1. Protein Expr. Purif. **65:**66–76.
15. **Gescher, J. S., C. D. Cordova, and A. M. Spormann.** 2008. Dissimilatory iron reduction in *Escherichia coli*: identification of CymA of *Shewanella oneidensis* and NapC of *E. coli* as ferric reductases. Mol. Microbiol. **68:**706–719.
16. **Gralnick, J. A., H. Vali, D. P. Lies, and D. K. Newman.** 2006. Extracellular respiration of dimethyl sulfoxide by *Shewanella oneidensis* strain MR-1. Proc. Natl. Acad. Sci. U. S. A. **103:**4669–4674.
17. **Hartshorne, R. S., et al.** 2007. A dedicated haem lyase is required for the maturation of a novel bacterial cytochrome c with unconventional covalent haem binding. Mol. Microbiol. **64:**1049–1060.
18. **Hartshorne, S., D. J. Richardson, and J. Simon.** 2006. Multiple haem lyase genes indicate substrate specificity in cytochrome c biogenesis. Biochem. Soc. Trans. **34:**146–149.

18a. **Heeb, S., Y. Itoh, T. Nishijyo, U. Schnider, C. Keel, J. Wade, U. Walsh, F. O'Gara, and D. Haas.** 2000. Small, stable shuttle vectors, based on the minimal pVS1 replicon for use in gram-negative, plant-associated bacteria. Mol. Plant Microbe Interact. **13:**232–237.

19. **Heidelberg, J. F., et al.** 2002. Genome sequence of the dissimilatory metal ion-reducing bacteriaum *Shewanella oneidensis*. Nature Biotechnol. **20:**1118–1123.
20. **Hensel, M., A. P. Hinsley, T. Nikolaus, G. Sawers, and B. C. Berks.** 1999. The genetic basis of tetrathionate respiration in *Salmonella* Typhimurium. Mol. Microbiol. **32:**275–287.
21. **Hussain, H., J. Grove, L. Griffiths, S. Busby, and J. Cole.** 1994. A seven-gene operon essential for formate-dependent nitrite reduction to ammonia by enteric bacteria. Mol. Microbiol. **12:**153–163.
22. **Jormakka, M., et al.** 2008. Molecular mechanism of energy conservation in polysulfide respiration. Nat. Struct. Mol. Biol. **15:**730–737.
23. **Kallastu, A., R. Horak, and M. Kivisaar.** 1998. Identification and characterization of IS1411, a new insertion sequence which causes transcriptional activation of the phenol degradation genes in *Pseudomonas putida*. J. Bacteriol. **180:**5306–5312.
24. **Mahillon, J., and M. Chandler.** 1998. Insertion sequences. Microbiol. Mol. Biol. Rev. **62:**725–774.
25. **Maki, H., and K. Murakami.** 1997. Formation of potent hybrid promoters of the mutant *llm* gene by IS256 transposition in methicillin-resistant *Staphylococcus aureus*. J. Bacteriol. **179:**6944–6948.
26. **McGuirl, M. A., J. A. Bollinger, N. Cosper, R. A. Scott, and D. M. Dooley.** 2001. Expression, purification, and characterization of NosL, a novel Cu(I) protein of the nitrous oxide reductase (nos) gene cluster. J. Biol. Inorg. Chem. **6:**189–195.
27. **Methe, B. A., et al.** 2003. Genome of *Geobacter sulfurreducens*: metal reduction in subsurface environments. Science **302:**1967–1969.
28. **Morris, C. J., et al.** 1994. Purification and properties of a novel cytochrome: flavocytochrome c from Shewanella putrefaciens. Biochem. J. **302**(pt. 2)**:** 587–593.
29. **Munch, R., et al.** 2005. Virtual Footprint and PRODORIC: an integrative framework for regulon prediction in prokaryotes. Bioinformatics **21:**4187–4189.
30. **Myers, C. R., and J. M. Myers.** 1997. Cloning and sequence of cymA, a gene encoding a tetraheme cytochrome c required for reduction of iron(III), fumarate, and nitrate by *Shewanella putrefaciens* MR-1. J. Bacteriol. **179:** 1143–1152.
31. **Myers, C. R., and J. M. Myers.** 1993. Ferric reductase is associated with the membranes of anaerobically grown *Shewanella putrefaciens* MR-1. FEMS Microbiol. Lett. **108:**15–22.
32. **Myers, J. M., and C. R. Myers.** 2000. Role of the tetraheme cytochrome CymA in anaerobic electron transport in cells of *Shewanella putrefaciens* MR-1 with normal levels of menaquinone. J. Bacteriol. **182:**67–75.
33. **Myers, C. R., and K. H. Nealson.** 1988. Bacterial manganese reduction and growth with manganese oxide as the sole electron acceptor. Science **240:** 1319–1321.
34. **Nealson, K. H., A. Belz, and B. McKee.** 2002. Breathing metals as a way of life: geobiology in action. Antonie Van Leeuwenhoek **81:**215–222.
35. **Nurk, A., A. Tamm, R. Horak, and M. Kivisaar.** 1993. In-vivo-generated fusion promoters in *Pseudomonas putida*. Gene **127:**23–29.
36. **Pitts, K. E., et al.** 2003. Characterization of the *Shewanella oneidensis* MR-1 decaheme cytochrome MtrA: expression in Escherichia coli confers the ability to reduce soluble Fe(III) chelates. J. Biol. Chem. **278:**27758–27765.
37. **Reynolds, A. E., J. Felton, and A. Wright.** 1981. Insertion of DNA activates the cryptic bgl operon in *E. coli* K12. Nature **293:**625–629.
38. **Rodrigues, M. L., T. F. Oliveira, I. A. Pereira, and M. Archer.** 2006. X-ray structure of the membrane-bound cytochrome c quinol dehydrogenase NrfH reveals novel haem coordination. EMBO J. **25:**5951–5960.
39. **Romine, M. F., T. S. Carlson, A. D. Norbeck, L. A. McCue, and M. S. Lipton.** 2008. Identification of mobile elements and pseudogenes in the *Shewanella oneidensis* MR-1 genome. Appl. Environ. Microbiol. **74:**3257–3265.
40. **Ruebush, S. S., S. L. Brantley, and M. Tien.** 2006. Reduction of soluble and insoluble iron forms by membrane fractions of *Shewanella oneidensis* grown under aerobic and anaerobic conditions. Appl. Environ. Microbiol. **72:**2925–2935.
41. **Schuetz, B., M. Schicklberger, J. Kuermann, A. M. Spormann, and J. Gescher.** 2009. Periplasmic electron transfer via the c-type cytochromes MtrA and FccA of *Shewanella oneidensis* MR-1. Appl. Environ. Microbiol. **75:**7789–7796.
42. **Schwalb, C., S. K. Chapman, and G. A. Reid.** 2003. The tetraheme cytochrome CymA is required for anaerobic respiration with dimethyl sulfoxide and nitrite in *Shewanella oneidensis*. Biochemistry **42:**9491–9497.
43. **Shirodkar, S., S. Reed, M. Romine, and D. Saffarini.** 2010. The octahaem SirA catalyses dissimilatory sulfite reduction in *Shewanella oneidensis* MR-1. Environ. Microbiol. [Epub ahead of print.] doi:10.1111/j.1462-2920.2010.02313.x.
44. **Simon, J., and M. Kern.** 2008. Quinone-reactive proteins devoid of haem b form widespread membrane-bound electron transport modules in bacterial respiration. Biochem. Soc. Trans. **36:**1011–1016.
45. **Simon, J., R. J. van Spanning, and D. J. Richardson.** 2008. The organisation of proton motive and non-proton motive redox loops in prokaryotic respiratory systems. Biochim. Biophys. Acta **1777:**1480–1490.
46. **Thomas, S. H., et al.** 2008. The mosaic genome of *Anaeromyxobacter dehalogenans* strain 2CP-C suggests an aerobic common ancestor to the delta-proteobacteria. PLoS One **3:**e2103.
47. **Thormann, K. M., et al.** 2006. Control of formation and cellular detachment from *Shewanella oneidensis* MR-1 biofilms by cyclic di-GMP. J. Bacteriol. **188:**2681–2691.
48. **Thormann, K. M., R. M. Saville, S. Shukla, and A. M. Spormann.** 2005. Induction of rapid detachment in *Shewanella oneidensis* MR-1 biofilms. J. Bacteriol. **187:**1014–1021.
49. **Vandesompele, J., et al.** 2002. Accurate normalization of real-time quantitative RT-PCR data by geometric averaging of multiple internal control genes. Genome Biol. **3:**RESEARCH0034.

49a. **Venkateswaran, K., D. P. Moser, M. E. Dollhopf, D. P. Lies, D. A. Saffarini, B. J. MacGregor, D. B. Ringelberg, D. C. White, M. Nishijima, H. Sano, J. Burghardt, E. Stackebrandt, and K. H. Nealson.** 1999. Polyphasic taxonomy of the genus Shewanella and description of Shewanella oneidensis sp. nov. Int. J. Syst. Bacteriol. **49:**705–724.

49b. **Wan, X. F., N. C. Verberkmoes, L. A. McCue, D. Stanek, H. Connelly, L. J. Hauser, L. Wu, X. Liu, T. Yan, A. Leaphart, R. L. Hettich, J. Zhou, and D. K. Thompson.** 2004. Transcriptomic and proteomic characterization of the Fur modulon in the metal-reducing bacterium *Shewanella oneidensis*. J. Bacteriol. **186:**8385–8400.

50. **Yang, Y., et al.** 2008. Characterization of the *Shewanella oneidensis* Fur gene: roles in iron and acid tolerance response. BMC Genomics **9**(Suppl. 1)**:**S11.
51. **Zhang, X., and H. Bremer.** 1995. Control of the *Escherichia coli rrnB* P1 promoter strength by ppGpp. J. Biol. Chem. **270:**11181–11189.
52. **Zumft, W. G.** 2005. Biogenesis of the bacterial respiratory CuA, Cu-S enzyme nitrous oxide reductase. J. Mol. Microbiol. Biotechnol. **10:**154–166.